METHODOLOGIES TO ASSESS AND QUANTIFY EARTHQUAKE DAMAGE: A DAMAGE ASSESSMENT CASE STUDY OF THE BNZ BUILDING IN WELLINGTON FOLLOWING THE 2016 KAIKOURA EARTHQUAKE

Umair Siddiqui, Will Parker, Robert Davey, Simon Therkleson[1], Quincy Ma[2]

[[1]WSP Opus, [2]University of Auckland]

ABSTRACT

Following damaging earthquakes, building owners need to understand the nature and extent of damage, the effect on the operations of their buildings, the residual capacity of the building to withstand another earthquake and aftershock, and the scope and cost of any required restoration work. Whilst the MBIE Residential Guidance provides technical solutions for repairing and rebuilding houses affected by 2010-11 Canterbury Earthquakes, there is presently limited authoritative guidance and benchmarks on how to assess and repair commercial properties damaged during earthquakes.

This paper outlines the approaches taken for the damage assessment of the BNZ building on Waterloo Quay in Wellington. The building was severely damaged in the 2016 Kaikōura Earthquake. The four methods used in our assessment include; the 'Japanese' guidelines method using residual crack widths, the cyclic fatigue demands on the global structure and the reinforcing steel strain and the seismic damage indices and each have their own limitations. The level of damage indicated by each method varies however all the methods are consistent in identifying the trend of damage to the building which correlates well with the observations.

BUILDING DESCRIPTION

The BNZ Harbour Quays building is a modern six-storey commercial office building constructed c. 2006 and located at 60 Waterloo Quay on the Wellington waterfront. The structure comprises three structurally independent reinforced concrete framed buildings, referred in this paper as 'Piers' which are separated by two full-height atria spaces. Piers 1 and 2, and piers 2 and 3 are interconnected via steel 'link bridges' at both ends of each level to tie the three piers together in the longitudinal (North-South) direction.

Reinforced concrete moment resisting frames (MRFs) provide the main lateral resisting system with a pair of perimeter MRF in the longitudinal and transverse directions of each of the three piers. The frames consist of precast concrete beams with in-situ column and joint elements designed and detailed for high ductility with μ=6.0 in both directions. The spacing between longitudinal frame columns varies between 5.4 to 6.0 meters, whereas in the transverse frames the columns are 8.1 meters apart. The typical floor system is 400 mm thick hollowcore slab spanning 16.8 meters between the transverse frames with a topping slab thickness of 70mm.

The building foundations comprise 12 - 15 m deep bored concrete piles with varying diameters of between 800 mm to 1500 mm, together with some concrete-filled steel tube driven piles. The piles are tied together at ground level by reinforced concrete ground beams.

The BNZ building is founded on reclaimed land which is approximately flat with ground surface level approximately 2 m above mean sea level. The depth of the reclamation fill varies from 2 m to 5 - 8 m.

The detailed description of the building is provided in [6]. Figure 1 shows the west elevation as visible from the Waterloo Quay frontage and a typical plan layout of the building.

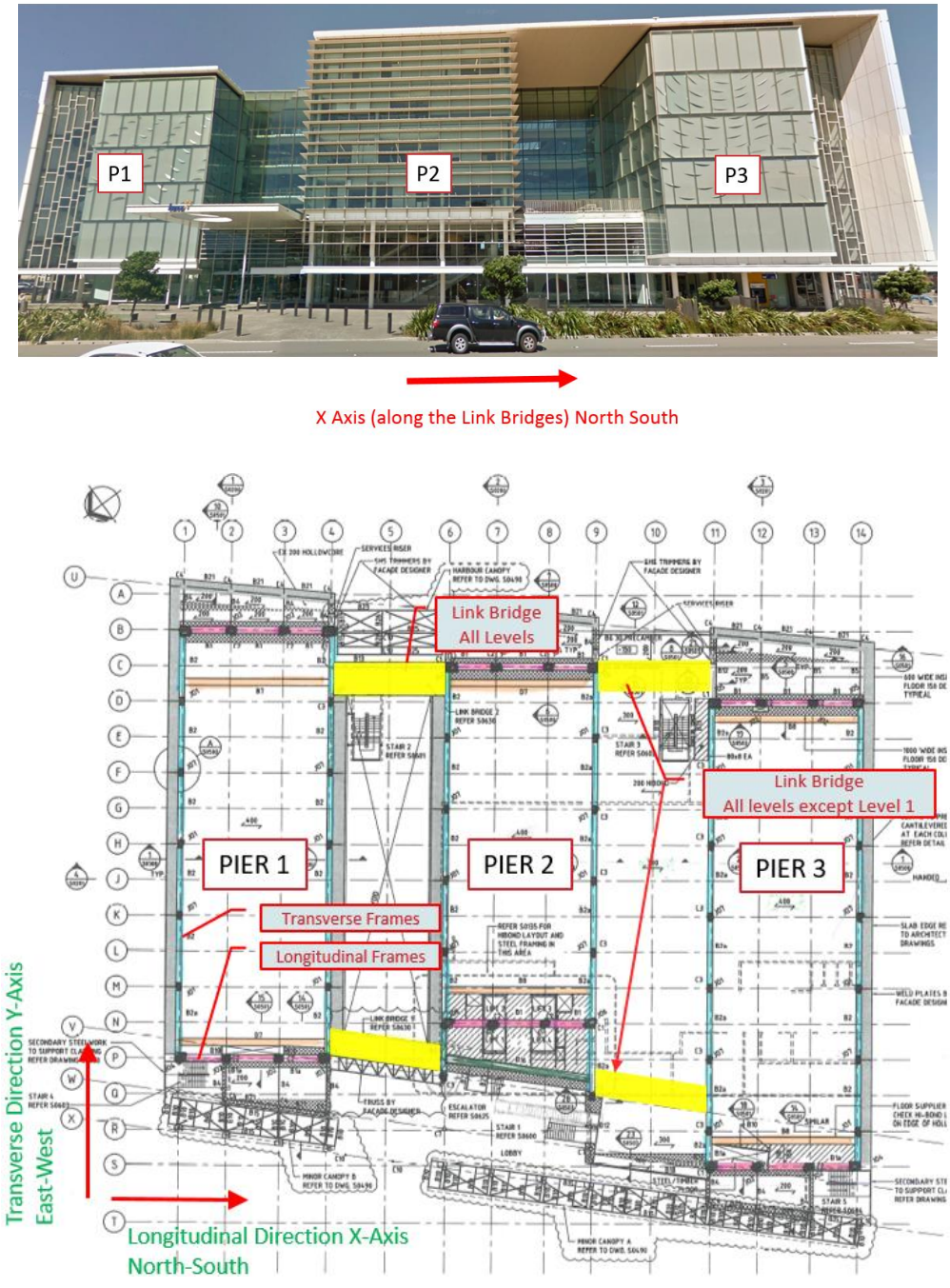

Figure 1. West Elevation (Waterloo Quay Side) and Plan at Level 2

DAMAGE – A BYPRODUCT OF CAPACITY DESIGN in NZ STANDARDS

The modern practice of capacity structural design to limit states for seismic loads is such that structures can withstand only minor levels of seismic shaking within the elastic range, termed the 'Serviceability Limit State' (SLS). For normal buildings not designed for crowds or post-disaster function, the SLS level shaking is a one in 25 year earthquake event. For shaking demands higher than SLS, energy is dissipated through inelastic irreversible deformation at designated regions of structural members. Whist this ensures the building will have low probability of collapse or becoming unstable, this effectively leads to permanent member damage.

The current New Zealand design standards ([3] and [4]) allow the reduction of seismic demands by exploiting ductility. This is implemented by reducing the design action by μ as a 'force-reduction factor' (k_μ) as well as further reduce the Ultimate Limit State (ULS) demands by the 'structural performance factor' (S_p).

In the context of the BNZ building during the November 2016 Kaikōura earthquake, the building experienced seismic demands equal to or in excess of the ULS seismic demands as shown in Figure 2. Figure 2 presents the elastic acceleration response spectra for each pier. The solid red and black lines represent the transverse (E-W) direction free field and base demand respectively, and the dotted lines represent the corresponding demand in the longitudinal (N-S) direction. The green vertical lines indicate the fundamental period of the building in the two direction as determined from the modal analysis. The blue solid and dashed lines represent the ULS elastic and design spectral ordinates as per NZS 1170.5 respectively.

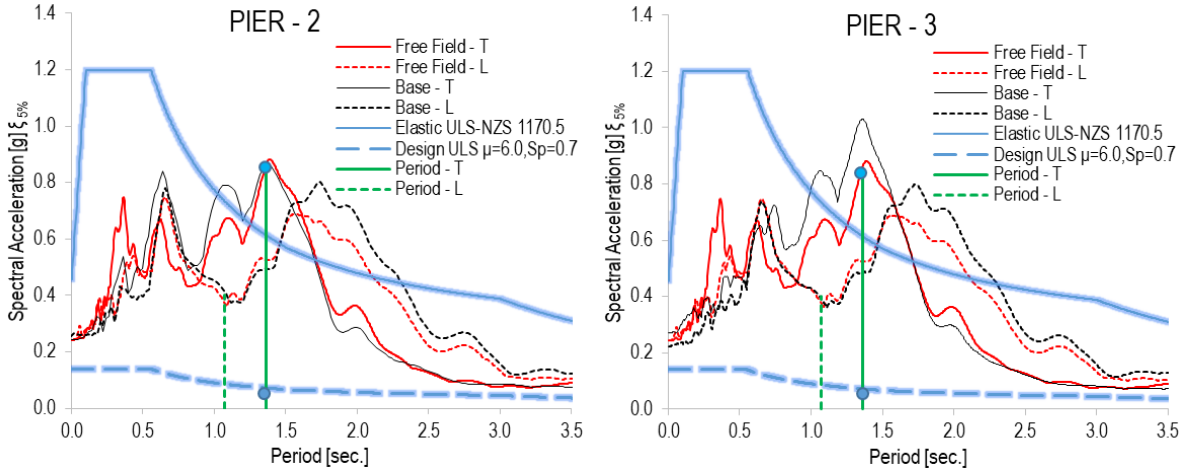

Figure 2. Elastic Acceleration Response Spectra Comparison for Piers 2 & 3

Comparing the plots for both piers and for the base and free field spectra, it can be observed that the intensity of ground shaking has exceeded the ULS demand in the transverse direction for periods between 1.0 to 1.5 seconds. The elastic base shear demands were nearly eight times higher than the designed base shear (as per [3] by taking k_μ =6.0 and S_p = 0.7)

In terms of displacement response, Figure 3 plots the peak recorded displacements for the three piers from accelerometer records on the building. Also shown are the estimated yield displacement profile from a pushover analysis, and the peak displacements from an ETABS non-linear 3D time history analysis using recorded Kaikōura accelerometer records. The peak roof displacement ductility demands during Kaikōura earthquake ranged between 3.0 and 4.2 for the three piers in the transverse direction frames where most damage was observed. The

ductility demands for lower stories is expected to be higher where most of the plastic deformations in the frames took place.

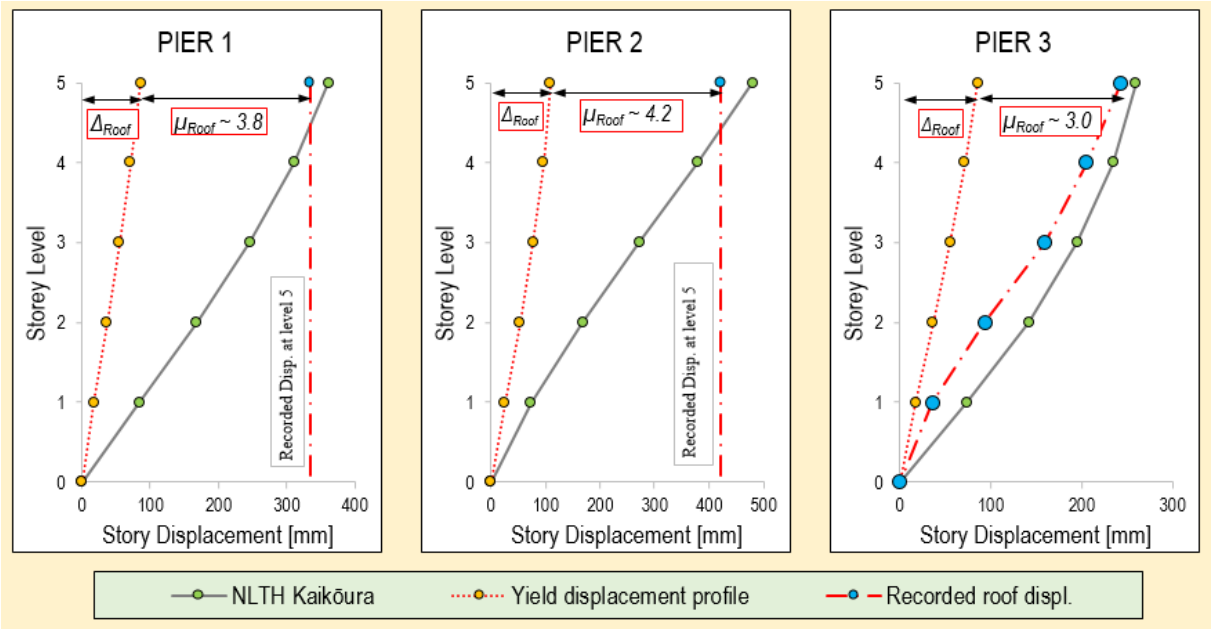

Figure 3. Ductility demands at roof level in each pier in transverse (EW) direction

OBJECTIVES OF DAMAGE EVALUATION ON THE BNZ BUILDING

In 2017, WSP Opus was engaged by Harbour Quays F1F2 Ltd to carry out an independent damage assessment in accordance with the following instructions:

- *For the purposes of this Damage Assessment, the Property has been damaged if there has been a physical alteration or change to the Property, not necessarily permanent or irreparable, which impairs its value or usefulness. This is a generally accepted definition of 'damage'.*
- *Record all damage to and at the Property, including structural, utility, amenity and aesthetic damage.*
- *Provide a summary of the observed damage.*
- *Provide a summary of the assessed damage, being damage that cannot be seen or is covered up, including the basis for that assessment.*

The investigations and testing of reinforcement were carried out on the building however, the extent of investigations was limited. The accelerometer recordings were available only on Pier 3, which was observed to be the least damaged. Hence extrapolation of structural damage to encompass the entire building through assessment was the main objective in light of provided definition of damage.

Investigation work was carried out on site by Beca and Fletcher Construction [5] prior to WSP Opus' involvement. Assessment of the precast concrete construction has been carried out by Professor Des Bull under an external engagement. WSP Opus did not carry out any intrusive investigations and the assessment relied on the factual information provided by Beca, Fletcher Construction, and the Harbour Quays F1F2 Ltd.

AVAILABLE INFORMATION FROM THE OBSERVED BUILDING DAMAGE

Following the November 2016 Kaikōura Earthquake, the BNZ building was subject to extensive investigations by several parties to determine the extent of damage. The information collected and used herein for damage evaluation is from the sources outlined in *Table 1*.

Table 1: List of investigations and source of information

Investigation	Collected Data
Non-intrusive visual inspection	Crack mapping to beams, columns and floor units. [conducted by Beca and independently verified by WSP Opus on a sample of data]
Accelerometer Instrumentation Records	Recorded acceleration time histories at the base and floor levels. [Data is courtesy of GNS Science and University of Canterbury]
Material Testing	Tensile tests, Leeb and Vickers Hardness testing on reinforcement of the topping slab and the bottom reinforcement of beams to determine loss of strain capacity. [Conducted by Holmes Group and University of Canterbury]
Verticality Survey and Laser Point Cloud Survey	Column verticality, global settlement, floor level sagging. [Conducted by Beca and WSP Opus]

The data from the investigation is presented in the paper Siddiqui et al. in [6].

DAMAGE ASSESSMENT

The evaluation of damage to the BNZ Building from the 2016 Kaikoura earthquake has used different approaches available in both literature and international guidelines. The primary objective was to investigate and quantify the extent of damage to the main lateral load resisting moment frames. Depending on the damage assessment methodology, the input utilizes the data collected from investigations including storey displacements using accelerometer records; global and member deformations from the nonlinear time history and pushover analyses; and visual damage observations and crack mapping.

The following methods outlined in Table 2 were employed to assess and quantify the damage to the building structure:

Table 2: Methods used for Damage Evaluation

Method	Investigation	Collected Data
1	Evaluation of lost capacity in accordance with Japanese Guidelines	Crack mapping in primary frames
2	Evaluation of cyclic fatigue demand on the structure	Displacement time histories from accelerometer records
3	Evaluation of low cycle fatigue damage to reinforcing bars in primary frames	Cyclic strain demands on the reinforcement from non-linear time history analysis (NLTH)
4	Evaluation of seismic damage indices	Global and local seismic response parameters including; peak ductility demands, roof displacement and storey drifts, cyclic strain demands on plastic hinge regions from records and NLTH.

Method – 1: Evaluation of Seismic Residual Capacity in accordance with Japanese Guidelines

A simple damage evaluation of the BNZ building has been carried out to the Japanese Guideline [7]. This methodology is further described by Maeda et al. [8] and highlighted by Sarrafzadeh et al. [9] in the 2017 NZSEE Bulletin.

The Guidelines set out a method for evaluating the residual seismic capacity of reinforced concrete structures post-earthquake, given by an R-index. The guideline is based on calibration between tested data and observed damage to identify the appropriate damage class and then assign a seismic capacity reduction factor '*η'* to account for the reduction in capacity post-seismic event. The ratio of cumulative capacities pre and post the seismic event is termed as the R-index or the reduction factor for the entire frame or structure.

The R-index is defined as;

$$R = \frac{\sum_{j=0}^{5} B_j}{B_{org}} \times 100 \ (\%)$$

where;

B_j is the normalized residual seismic capacity of the structural member in damage class *j*,
B_{org} is normalized seismic capacity before the earthquake damage
and the seismic capacity reduction factor '*η*' for ductile beams estimates the residual capacity based on the damage class as per Table 3.

Table 3. Seismic capacity reduction factors 'η' for different member types from [8]

Damage class	RC Column			RC Wall		RC Beam	
	Shear	*Shear-Flexural*	*Flexural*	*Shear*	*Flexural*	*Shear*	*Flexural*
Ⅰ	0.95	0.95	0.95	0.95	0.95	0.95	0.95
Ⅱ	0.6	0.7	0.75	0.6	0.7	0.7	0.75
Ⅲ	0.3	0.4	0.5	0.3	0.4	0.4	0.5
Ⅳ	0	0.1	0.2	0	0.1	0.1	0.2
Ⅴ	0	0	0	0	0	0	0

The damage is defined as the percent capacity loss = 1 – *η* (%)

Damage class and type of damage

There are five damage classes defined in [7]: I (least damage), II, III, IV and V (most damage). Table 4 provides the definition of each damage class with its associated residual crack width.

Table 4. Definition of damage classes of structural members (from [7])

Damage Class	Observed Damage on Structural Members
I	Some cracks found with crack widths smaller than 0.2mm
II	Cracks of 0.2 – 1.0 mm width are found
III	Heavy cracking with crack width of 1 – 2 mm are found. Some spalling of concrete is observed
IV	Many heavy cracks are found with crack widths larger than 2.0mm. Reinforcing bars are exposed due to spalling of the covering concrete
V	Buckling of reinforcement, crushing of concrete and vertical deformation of columns and/or shearwalls are found. Side-sway, subsidence of upper floors and/or fracture of reinforcing bars are observed in some areas

Table 5 summarizes the damage percentages calculated for two cases; 1) average damage percentage for all storeys and 2) average damage percentage for lower three stories. This is performed to understand the damage to lower storeys which are primarily contributing for the frame ductility and subject to higher ductility demand.

Table 5. R-index and damage percentages using crack mapping data

Pier	Direction	Grid	R-index (for all storeys)	Damage (%)	Damage Class	R-index (for bottom 3 storeys)	Damage (%)	Damage Class
1	Transverse	1	0.54	46%	Severe	0.42	58%	Severe
		4	0.56	44%	Severe	0.42	58%	Severe
	Longitudinal	B	0.80	20%	Moderate to Minor	0.76	24%	Moderate
		P	0.81	21%	Moderate to Minor	0.77	23%	Moderate
2	Transverse	6	0.50	50%	Severe	0.37	63%	Severe
		9	0.48	52%	Severe	0.33	67%	Severe
	Longitudinal	C	0.77	23%	Moderate	0.79	21%	Moderate
		N	Not enough crack mapping data					
3	Transverse	11	0.65	35%	Moderate	0.59	41%	Moderate to Severe
		14	0.66	34%	Moderate	0.61	39%	Moderate to Severe
	Longitudinal	D	0.82	18%	Moderate to Minor	0.79	21%	Moderate
		S	0.76	24%	Moderate	0.72	28%	Moderate

Verification of Capacity Reduction Factors *'η'* for Frames using NLTH Results

The theory underpinning the Guideline [7] is applied to compare the damage levels observed with the damage predicted by the analytical structural model. This is achieved by calculating the '*η*' factor for the concrete moment-resisting-frames of the building using the ratio of dissipated to total energy dissipation capacity. Figure 4 presents the basic concept of the '*η*' factor used.

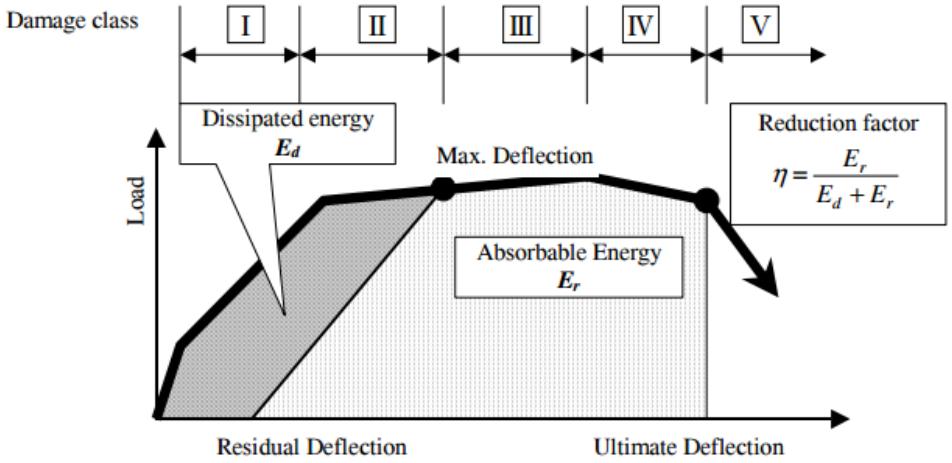

Figure 4: Concept of Seismic Capacity Reduction Factor, '*η*' (reproduced from [7])

The ratio of remaining energy dissipation capacity '$E_{remaining}$' vs the total energy dissipation capacity '$E_{Capacity}$' is used to calculated the seismic capacity reduction factor '*η'* for the moment resisting frames of each pier as follows;

$$\eta = \frac{E_{Capacity} - E_{Dissipated}}{E_{Capacity}} = \frac{E_{remaining}}{E_{total}}$$

An example from Pier 1 is shown in Figure 5 where the hysteresis response curves from NLTH are plotted in light blue. The estimated energy dissipated during the earthquake is indicated with solid blue solid line forming the flag shaped envelope of the hysteresis curve for each seismic frame. The capacity pushover curve for the respective frame obtained from 3D non-linear pushover analysis of the building is plotted in dotted red lines which is used to calculate the total energy dissipation capacity E_{total}.

The total available or 'undamaged' energy dissipation capacity, E_{total}, is estimated by calculating the total area under the force displacement capacity curve for each frame. The capacity curve is established based on a 3D non-linear pushover analysis of the building in each direction up to a maximum displacement of approximately 680mm at Level 5. This displacement correlates to a displacement point in the pushover curve where the plastic strains in the reinforcing within the moment frame beams are in the range of 6.0-8.5% for at least three or more storeys which is taken as the threshold for low cyclic fatigue failure in the beam reinforcing bars in this assessment as per the New Zealand guidelines [9].

The dissipated energy, $E_{Dissipated}$, is estimated by calculating the area within the effective maximum flag shaped hysteresis response obtained from the non-linear time history analysis of the building using the level 5 displacement and the reactions at the base of each respective Pier. Note that outlying areas which exceed the push over capacity curve have been excluded from the estimated response data to improve consistency.

The capacity reduction factor '*η'* is calculated separately for each direction envelope i.e. forward and reverse displacement cycle and the final factor for reduction in capacity is taken as the average of the reduction factors in the forward and reverse cycles.

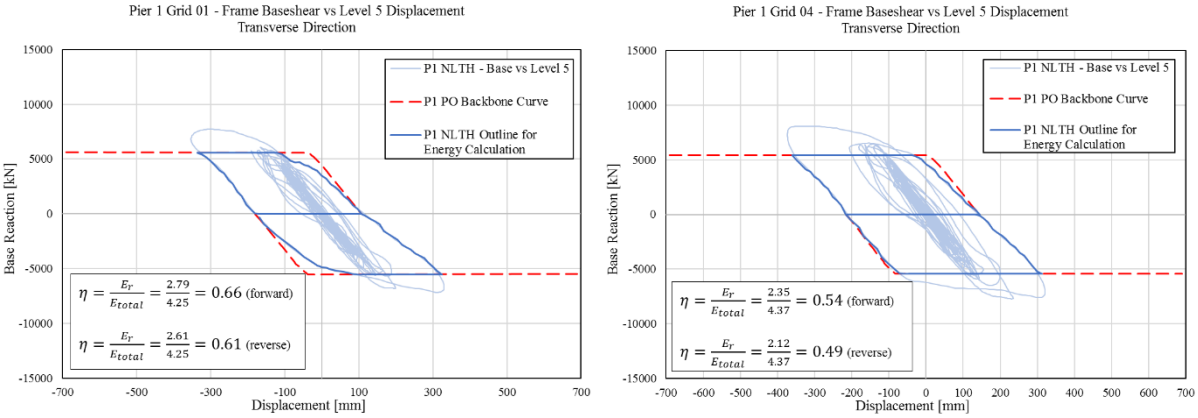

Figure 5. Pier 1 Transverse Frames along Grid 1 & 4- Hysteresis and Pushover Curves and '*η'* factors

The results for all the frames are summarized in Table 9 for all frames.

Assumptions and Limitations

The following points should be considered when comparing these results with other methods:

- The purpose of calculating the global capacity reduction factor '*η*' using NLTH results is to use it as a means of verification of the damage in the frames globally. The objective is not to provide an extension of the existing procedure or to propose a new method of damage evaluation.
- The dissipated energy calculation is based on the maximum envelope and does not consider multiple cycles post-yield. The method does not explicitly take in to account cyclic fatigue damage.
- The pushover analysis which is used to determine the original capacity for each frame does not account for bi-directional effects which are included in the time history analysis.
- The damage is expected to provide a global indication of damage however since the top level drifts are not representative of all levels, the damage at certain levels is expected to be higher than that estimated using this method.
- Calibration of the model with the building response is critical for this method which has been performed using recorded accelerometer data and sensitivity studies on the plastic hinge behaviour of the beams. The detailed description of the analytical studies conducted on the BNZ building is presented in the paper by Siddiqui, et al [6].

Table 6. Evaluated η factors using NLTH results

Pier	Direction	Grid	η -factor (for frame)	Damage (%)	Damage Class to [5]	Damage Extent
1	Trans.	1	0.63	37%	III	Moderate
		4	0.51	49%	IV	Moderate to Severe
	Long.	B	0.83	17%	II	Moderate to Minor
		P	0.65	35%	III	Moderate
2	Trans.	6	0.43	57%	IV	Severe
		9	0.36	64%	IV	Severe
	Long.	C	0.82	18%	II	Moderate to Minor
		N	0.67	33%	III	Moderate
3	Trans.	11	0.83	17%	II	Moderate to Minor
		14	0.84	16%	II	Moderate to Minor
	Long.	D	0.87	13%	II	Minor
		S	0.63	37%	III	Moderate

Method – 2: Damage under Cyclic Loading using Instrumented Data for Displacement Time-Histories

The cyclic fatigue damage on the reinforced concrete moment resisting frames of the building has been evaluated using the procedure proposed by [10] and [11]. The method is based on evaluating the cyclic fatigue life of a ductile structure which has been consumed by an earthquake (or an aftershock) when it has undergone vibrations or "swayed" over several cycles [12]. The cyclic fatigue demand in a reinforced concrete structure designed to respond in a ductile manner is imposed when during a seismic event the reinforcing steel undergoes

several cycles of strains beyond its elastic limit [13]. Although the post-yield strain capacity of reinforcing bars under monotonic loading in general is sufficiently large (where it can be up to 15%-20%), when several large reversed cycles of strain occur, the bars may sustain significant seismic induced fatigue damage. Such cyclic damage to the reinforcing bars is generally irreversible and is termed 'low-cycle fatigue'.

The fatigue damage is defined in terms of '*Damage Fraction'* (D_f) as the ratio of the number of cycles imposed by the earthquake loading (seismic demand) to the number of cycles to failure in the critical structural elements (the capacity).

The damage fraction 'D_f' can be given in terms of the effective number of cycles N_{eff} (or $2N_{eff}$ is equal to the number of peaks/reversals in the random loading history) to failure and the recorded peak displacement 'X_j' of the varying time history data as per equation below;

$$D_f = N_{eff} \left|\frac{\Delta_{pm}}{\Delta_{pf}}\right|^2 = \frac{1}{2} \times \sum_j \left|\frac{X_j}{\Delta_{pm}}\right|^2 \times \left|\frac{\Delta_{pm}}{\Delta_{pf}}\right|^2$$

In the equation above:
Δ_{pm} = Peak recorded displacement at the floor under consideration
Δ_{pf} = Peak floor displacement corresponding to fatigue failure in the main reinforcement bar.

The study [10] suggests that Δ_{pf} can be taken as the displacement value at the performance point of the structure. For example, ULS drifts at the code conformance level, or the target displacement at 100% ULS demand. For this assessment, the failure Δ_{pf} is defined as the displacement profile of the structure that will lead to reinforcement bar strains of up to 6 to 8.5% at either the top or bottom of the beam's plastic hinge zone for up to three or more storeys.

In this damage assessment, the above procedure is adopted by utilizing the displacement time histories from the recorded accelerometer data. Note that only pier P3, which is the least damaged pier, is instrumented sufficiently to get the inter-storey drift data to enable the computation of end-rotations and subsequent strains in the beam reinforcement while for the other two piers (P1 and P2) only the top storey displacement data was available.

The summary of damage evaluated based on cyclic fatigue demands is presented in Table 7 for the transverse and longitudinal frames of Pier 3. Damage percentage of longitudinal frame in Pier 3 is taken as representative of damage for all three piers as they are interconnected by means of link bridges with approximately equal longitudinal displacements.

Method – 3: Evaluation of Low Cycle Fatigue Damage on Reinforcement Bars in Beams

Method 3a: Cyclic Fatigue Damage in Reinforcing Bars using NLTH Results
The cyclic fatigue demand approach given in [13] is used here to evaluate the low-cycle fatigue damage in reinforcing bars at the Potential Plastic Hinge Zones (PPHZ) near the beam ends. The beam plastic rotation time histories from the NLTH analysis have been used to calculate the plastic rotations and the number of cycles of a specific rotation amplitude that the beam end has undergone.

The fatigue life relationship from [14] was tested to conform well to cyclic fatigue behaviour by [13] and it is adopted in our assessment as outlined below;

$$\Delta\varepsilon = 0.159\ (2N_f)^{-0.448}$$

The inverse to the number of cycles to failure 'N_f' may be defined as the damage for one cycle of loading 'D_{cycle}' at the total strain amplitude of '$\Delta\varepsilon$'. Thus, cumulating the damage of different cycles 'n_i' of varying strain amplitudes '$\Delta\varepsilon_i$' based on [14] can give the 'damage indicator' (D_f) as;

$$D_f = \sum_i \frac{n_i}{N_f(\Delta\varepsilon_i)}$$

The plastic strain values are calculated from plastic rotations as follows;

$$\phi_p = \frac{\theta_p}{L_p}$$

and

$$\Delta\varepsilon_i = \phi_p \times y_{NA} + \varepsilon_y$$

where;

L_p = Plastic hinge length,

θ_p = Plastic rotation from nonlinear time-history analysis,

y_{NA} = Depth of neutral axis from section analysis results for each beam.

Table 7. Fatigue Damage Summary for Transverse frame of Pier 3 and average for longitudinal frame along Grids D and S. (Method - 2)

Cyclic Fatigue Damage - Pier 3 Grid 14

Using Recorded Data

Level	Peak Drift at jth Cycle	Cycles of Amplitude Xj	Number of Eff. Cycles of Constant Amplitude	Story Damage fraction
	Xj	Nj	Neff	Σ Df
	mm			%
LVL 05	35	1.0	1.34	25%
	20	5.0		
	10	12.0		
LVL 04	45	2.0	3.45	31%
	30	4.0		
	20	9.0		
LVL 03	60	2.0	4.09	31%
	40	4.0		
	25	10.0		
LVL 02	55	2.0	5.34	39%
	40	4.0		
	25	8.0		
LVL 01	25	3.0	4.33	16%
	20	6.0		
	10	11.0		

Σ Df = 28%

Cyclic Fatigue Damage - Pier 3 Average for Longitudinal Frames

Using Recorded Data

Level	Peak Drift at jth Cycle	Cycles of Amplitude Xj	Number of Eff. Cycles of Constant Amplitude	Story Damage fraction
	Xj	Nj	Neff	Σ Df
	mm			%
LVL 05	30	0.0	1.23	8%
	15	7.0		
	10	13.0		
LVL 04	35	1.0	3.96	19%
	25	4.0		
	15	12.0		
LVL 03	55	1.0	3.62	24%
	35	5.0		
	20	12.0		
LVL 02	55	1.0	2.92	20%
	35	5.0		
	20	12.0		
LVL 01	45	1.0	2.33	9%
	20	6.0		
	10	12.0		

Σ Df 16%

The damage fraction values were sensitive to the strain values and plastic hinge lengths adopted in the lumped plasticity model. Therefore, a sensitivity analysis was conducted on a single bay frame with fibre-hinge model using SAP2000 to understand the distribution of plasticity for the beams loaded heavily under gravity loads. The results [6] indicated that due to large gravity loads the demands at the top of the beams are higher as compared to bottom of the beam resulting in so-called 'ratcheting' of the member. This was also supported by the observation and the downward sag of beams through survey. To account for that, a reduced plastic hinge based on the outcome of sensitivity analysis as compared to the literature values [10] was used to account for concentrated plasticity.

The results from the damage evaluation using the above approach for the structure following a simulated Kaikoura earthquake are presented as graphic overlays on the elevations of individual moment resisting frame (MRFs). Figure 6 presents the results for the transverse direction frame in Pier 2 (the most damaged pier) for illustration. The results in Figure 6 include;

- Damage Fraction D_{fi} The damage indicators for each beam at each joint (I-end and J-end) for top and bottom reinforcement.
- Peak plastic strains ε_p: The value of peak plastic strain amplitude observed by the first layer of reinforcement bars in the beam section.
- # of cycles of average strain: The number of cycles of average total strain experienced by the reinforcement. This is shown as a multiple of the yield strain 'ε_y'.
- Expected maximum crack width w_T: The expected maximum crack widths is evaluated for the joint region in accordance with the formulation in [15]. Note that the formulation for crack width is dependent on the mean concrete tensile strength f_{ctm} and hence it does not account for cold joints between the precast beams and the cast-in-situ joints at the bottom where f_{ctm} is expected to be zero.
- Observed residual crack width: provided for a comparison between the observed residual crack widths from damage mapping and the calculated expected maximum crack width near the PPHZs.
- Percent loss of strain capacity: The values of percentage loss of strain capacity are as reported by various material tests based on various testing procedures carried out on selected reinforcing bars.

The final damage percentage 'D_f' of the entire frame is calculated as a weighted average using triangular weighing function with maximum at the base storey.

$$D_f = \sum_{k=1}^{N} D_{fStorey}\, I_k$$

Where;

$$I_k = \frac{N+1-k}{N} \qquad and\ N: Number\ of\ storeys$$

The damage percentages for the frames in all three piers are summarized in Table 9.

Method – 3b: Cyclic Fatigue Damage on Reinforcing Bars using Recorded Data (Pier 3 only)

Similar to Method 3a, the damage indicators have been revaluated using the global storey displacements from the recorded instrumentation data to calculate the plastic deformation demands on the structure. The results are limited to Pier 3 as the storey drift records are only available for this Pier.

The global story displacements from the records 'Δ_{ult}' and the 'yield' displacements 'Δ_{yield}' from the pushover analysis are related to the plastic strains using geometric transformations i.e. $\Delta_{p\,i} \rightarrow \theta_{p\,i} \rightarrow \varphi_{p\,i} \rightarrow \varepsilon_{p\,i}$ where the parameters correspond to; the plastic storey drift (mm) [$\Delta_{p\,i} = \Delta_{ult} - \Delta_{yield}$], plastic beam rotations, plastic curvature near PPHZs and plastic strains in the reinforcement, respectively. The 'yield' displacements 'Δ_{yield}' refers to the storey displacement profile at the onset of yielding in beams obtained from the nonlinear static pushover analysis.

The calculation of damage indicator 'D_f' follows the same principal as for Method 3a in terms of calculations and definition of failure. The damage is estimated for a typical intermediate beam from the moment-resisting frame in Pier 3 with the results summarized in Table 9.

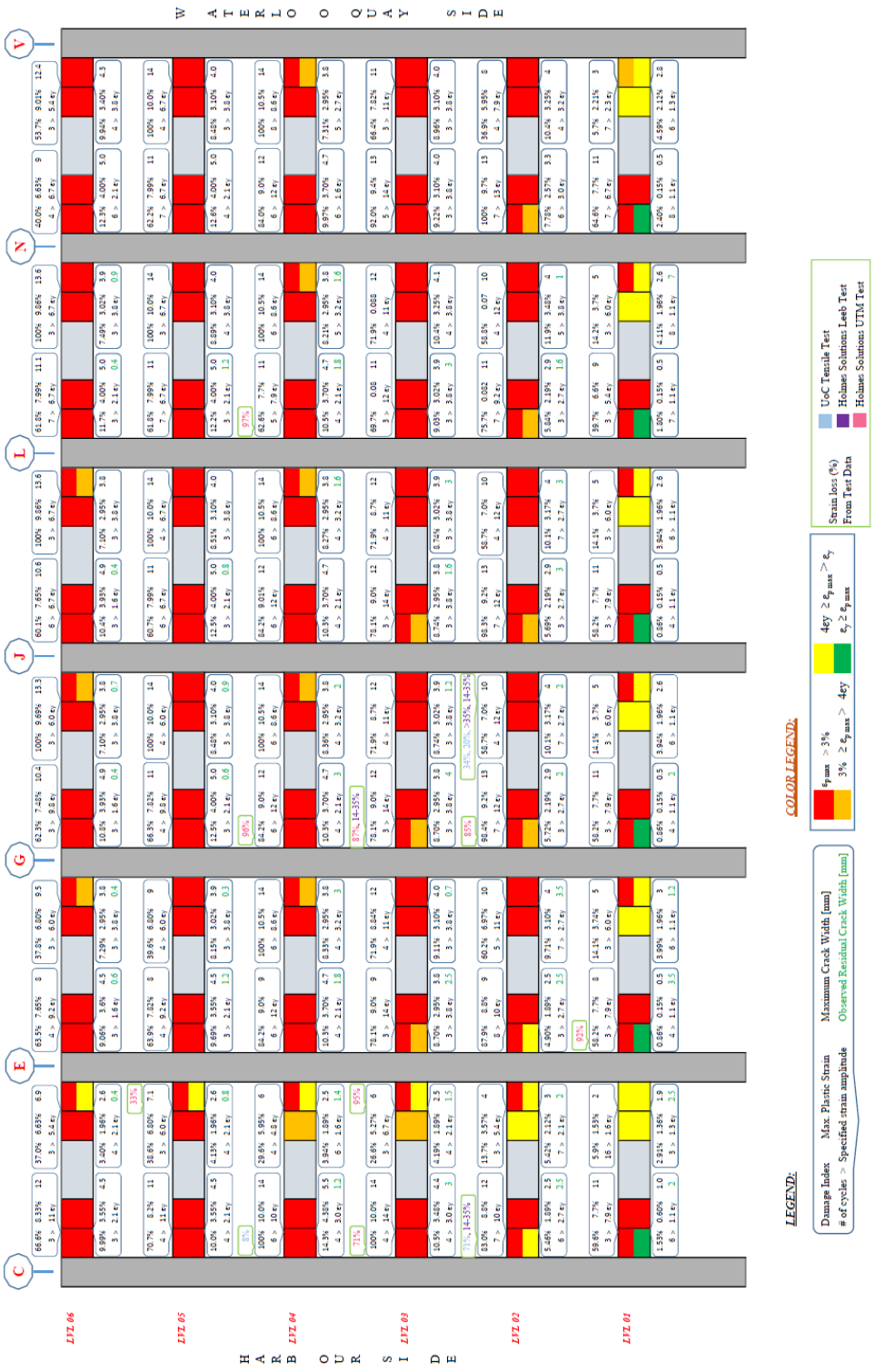

Figure 6 Elevation of Pier 2 Frame along Grid 09 – Damage Assessment Results

Method – 4: Seismic Damage Indices

A range of seismic damage indices were trialled to quantify the structural damage. The indices utilise several global and local inelastic deformation parameters. Damage Indices are dimensionless parameters, generally intended to range between 0 (for undamaged) and 1 (for collapsed) with intermediate values indicating the degree of damage to the structure [23]. The

global damage indices utilized peak global deformation parameters such as roof displacements or inter-story displacements to indicate damage to the structure, whereas local damage indices predict the damage in a member or at a joint. Local damage indicators are sometimes combined, for instance using a weighted average, to give an overall damage indication of the structure.

In reinforced concrete structures, seismic damage is a result of deformations beyond the elastic range. The sustained damage may be due to 'excessive deformation' (in-cyclic) or it may be accumulated damage due to 'cyclic load reversals'. The earliest and simplest damage indices are solely based on peak ductility demands, while recently, researchers have proposed damage indices that take in to account the cumulative effects by including hysteretic energy absorbed.

For this damage assessment, the damage indices shown in Table 8 have been used covering different categories of damage (noncumulative peak or cyclic) for local or global response parameters.

Table 8. Damage Indices Types used for Damage Assessment

Type	**Category**	**Main Parameter**	**Damage Model**
Local member damage	Non - Cumulative	Peak Ductility Demand on the Critical Member	*Roufaiel & Meyer 1987 [16]*
Storey damage	Cumulative	Cyclic Displacement Ductility	*Wang & Shah 1987 [17]*
Storey damage	Cumulative	Cyclic Hysteretic Energy Dissipation	*Gosain et al. 1977 [18]*
Local member damage	Combined	Peak Ductility Demand and Hysteretic Energy	*Park & Ang 1985 [19]*
Overall building damage	Global	Peak Roof Displacement	*Roufaiel & Meyer 1987 [20]*

Non-Cumulative *→ based only on the peak demands*
Cumulative *→ based only on cyclic accumulation of damage*
Combined *→ based on peak demand and cyclic accumulation*
Global *→ based on peak global responses e.g. roof displacement*

The results from the damage indices are shown in Figure 7. The results are representative of the damage in the worst damaged pier (Pier 2) in the transverse direction frames where damage percentage is calculated as a weighted average.

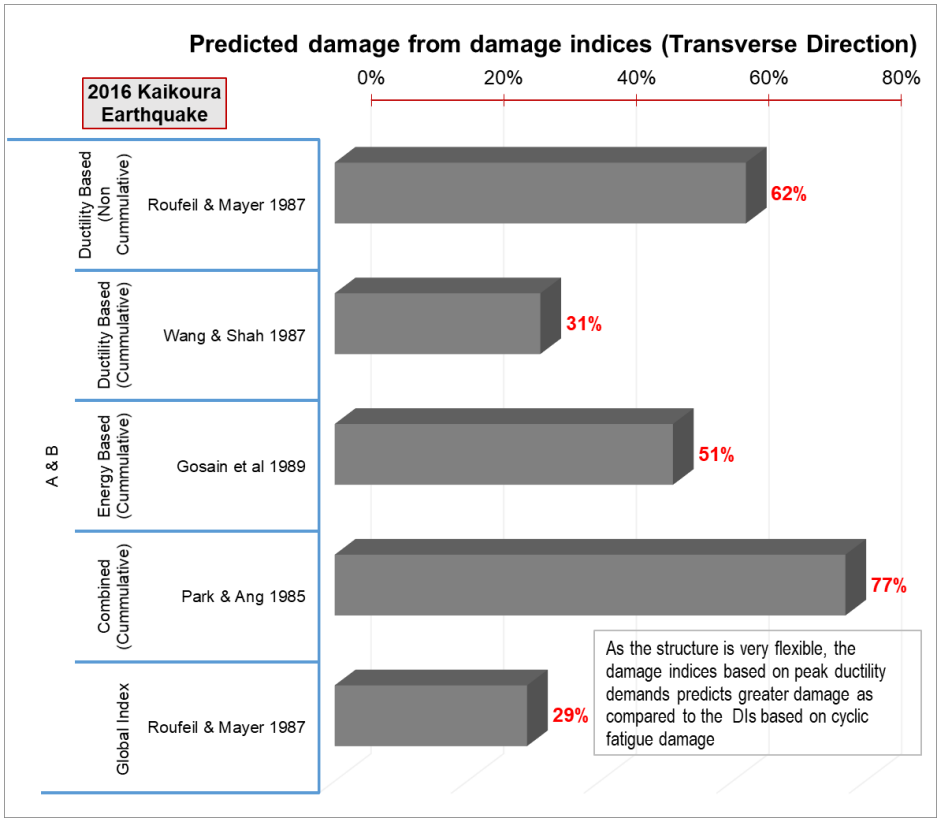

Figure 7 Predicted damage in transverse direction frames using damage indices

Extent of Plastic Deformation in the PPHZ Regions of Beams

The extent of plasticity in the beams has been determined as the average percentage of potential plastic hinge zones (PPHZs) within a frame which have undergone plastic (post-yield) deformation beyond a threshold using the results of nonlinear time history analysis. These results are collated to provide an indication of the behaviour and extent of damage that a ductile building undergoes when it has undergone ductility requirements beyond the serviceability limit state. There are four PPHZs in each beam, at the top and bottom of each end-zone. Two thresholds are used to measure the extent of plastic deformation in the PPHZs:

i) The maximum plastic (post-yield) strain in the reinforcement of plastic hinge region reaches or exceeds 2%.
ii) The average strain in the reinforcement undergoes 3 or more cycles of total strain amplitude equal to or more than 3 to 4 times the yield.

These thresholds have been selected based on the expectation that if a reinforcing bar on the tension face of the section (either top or bottom) has undergone strain values more than twice its yield strain values then the entire tensile region is expected to have undergone strains at least equal to the yield strain as well as sustained damage due to residual strain occurring over multiple cycles. Additionally, 2% of plastic strain is considered a sufficiently significant plastic deformation of reinforcement to cause cracking under cyclic loading. The plastic hinge lengths used to calculate these strains are based on literature values [21] and provide a conservative estimate of the extent of plasticity. Figure 8 presents the percentage of PPHZ exceeding plastic deformation thresholds relative to the total number of PPHZs.

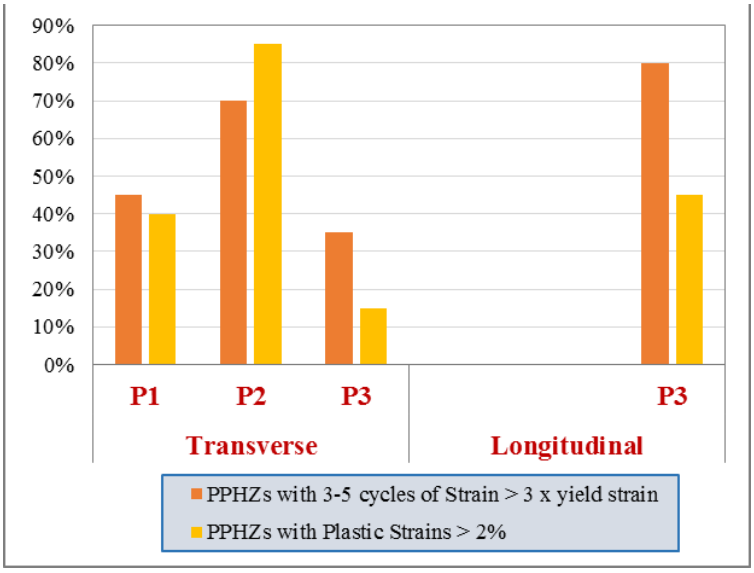

Figure 8. Extent of plastic deformation in PPHZs

SUMMARY OF DAMAGE ASSESSMENT

Table 9 summarizes the findings from each of the damage evaluation procedures carried out. The percentage ranges indicate the range between mean to peak values of respective damage as a percentage (%) for each pier.

Table 9. damage percentage summary using NLTH results

Direction	Pier	Japanese Guidelines method based on crack mapping	Japanese method based on dissipated / total energy	Cyclic fatigue damage of Structure	Cyclic fatigue damage to reinforcing bars based on reversing cycles of strains		Seismic Damage Indices	%age of Potential Plastic Hinge Zones with Plastic Deformations	
		Method - 1	Method - 1	Method - 2	Method - 3a	Method – 3b	Method - 4	-	-
Transverse Direction		**Procedure -->** Residual capacity using Japanese Guidelines **Input Data -->** Observed residual crackwidths	**Procedure -->** Evaluation of 'Capacity Reduction Factor' 'η' **Input Data -->** NLPO and NLTH 1) Capacity curves 2) Hysteresis curve	**Procedure -->** Low Cycle Fatigue damage using Mander et al method (2016) **Input Data -->** recorded story displacement time histories	**Procedure -->** Low Cycle Fatigue damage on reinforcement based on Mander et al method (1994) **Input Data -->** cyclic strain demands on rebars, Method 3a – NLTH, Method 3b – Records		**Procedure -->** Local and global damage indices **Input Data -->** global ductility, cumulative deformations	Total number of plastic hinge zones with 3 to 5 cycles of strains > 3 times ε_{yield} Total number of plastic hinge zones with max plastic strains > **2%** **Input Data -->** Beam plastic rotations and the number of cycles from NLTH	
	P1	40 - 45 %	37 - 50 %	**	*Top rebars:* 40 - 60 % *Bot rebars:* 5 - 10 %	**	Not assessed	45%	40%
	P2	50 - 55 %	55 - 65 %	**	*Top rebars:* 65 - 90 % *Bot rebars:* 10 - 15 %	**	30-77 %	70%	85%
	P3	30 - 35 %	16 - 17 %	28 - 35 %	*Top rebars:* 15 - 40 % *Bot rebars:* 5 - 10 %	*Top rebars:* 23 - 40 % *Bot rebars:* 7 - 12 %	Not assessed	35%	15%
Longitudinal Dir.	*All*	20 - 25 %	13 - 37 %	16 - 25 %	6 - 10 %	7 - 15 %	10-20 %	80%	45%

*** Recorded Data only available for Pier 3*

CONCLUSIONS

Across the spectrum of damages evaluated, the various methods indicate different levels of damage, however all the methods are consistent in identifying damage to all piers and the most damage to Pier 2, followed by Pier 1 and then Pier 3. These results correlate well with the observations. The main conclusions drawn from the case study are;

- The accelerometer records obtained from the instrumentation data proved beneficial in enabling the analysis, benchmarking and further extrapolation of building response.
- The damage indices based solely on global ductility demands (peak displacement ductility, peak roof displacement etc.) overestimate the level of damage for a flexible building.
- The damage methods do not take in to account the in-cycle member level 'ratcheting' in plastic hinge regions of beams loaded with large gravity loads.
- The results from damage methods based on degradation of plastic strain capacity of bars under cyclic loading are highly dependent on the plastic hinge length.
- Since most damage indices and cyclic fatigue damage methods are normalized to reach a value of unity for the damage state at failure, the definition of failure limit and defining what constitute a 'failure' is critical for the outcome.
- The damage levels evaluated from the different methods do not necessarily directly translate to cost of remediation since the aspect of reinstatement is very discrete and non-linear, e.g. 10% damage by any measure does not mean 10% of the cost of rebuild.

The results do vary between the different methods and each method has its own limitations. There is no one single method which can encompass all damage types and provide an accurate answer. In the absence of an authoritative guidance, our approach has been to use all available and applicable methods to indicate the damage and the overall results show a consistent trend.

ACKNOWLEDGEMENT

The authors acknowledge the contribution of Harbour Quays F1 F2 ltd., Beca Ltd., Holmes Consulting Group, Fletcher Construction and Dr. Reagan Chandramohan from University of Canterbury for the provision of factual investigation data on the building.

REFERENCES

[1] "The seismic assessment of existing buildings", Technical Guidelines for Engineering Assessments, July 2017, *MBIE - New Zealand.*

[2] Reagan C. et al., "Response of instrumented buildings under the 2016 Kaikoura earthquake", *Bulletin of the NZSEE, Vol.50, No. 2*, June 2017

[3] "Structure Design Actions – Part 5: Earthquake Actions – New Zealand", NZS 1170.5:2004 with A1 (2016), *New Zealand Standards*.

[4] Concrete Structure Standard" Part 1 and 2, NZS 3101:2006 with A3 (2017), *New Zealand Standards*.

[5] Beca Ltd., (2016-2017) *BEAM DAMAGE SUMMARY.pdf.*

[6] U. Siddiqui, W. Parker, R. Davey, S. Therkleson, “Seismic Response of BNZ Building in Wellington Following the 2016 Kaikoura Earthquake”, SESOC Conference 2019

[7] “Guideline for Post-Earthquake Damage Evaluation and Rehabilitation”. (in Japanese and translated to English), *The Japan Building Disaster Prevention Association (JBDPA)* (1991, revised in 2001 and 2015)

[8] Maeda M, Nishida T, Matsukawa K, Murakami M, “Revision of Guideline for Post-Earthquake Damage Evaluation of Reinforced Concrete Buildings in Japan.”, *16th World Conference on Earthquake Engineering - Chile*, 16WCEE, (2017).

[9] Sarrafzadeh M, Elwood J, Dhakal R, Ferner H, Pettinga D, Stannard M, Maeda M, Nakano Y, Mukai T, Koike T, “Performance of Reinforced Concrete Buildings in the 2016 Kumamoto Earthquakes and Seismic Design in Japan”, *Bulletin of the NZSEE, Vol.50, No. 3*, September 2017

[10] Mander J B, Rodgers G W, “Seismic Fatigue Damage Analysis: Procedures for Reinforced Concrete Structures”, (2016)

[11] Mander J B, et al., “Rapid Earthquake Loss Assessment: Stochastic Modelling and an Example of Cyclic Fatigue Damage from Christchurch”, (2016): *16th U.S.-Japan-New Zealand Workshop on the Improvement of Structural Engineering and Resiliency 2016.*

[12] Mander J B, Rodgers G W, “Cyclic fatigue demand on structures subject to the 2010-2011 Canterbury Earthquake Sequence”, *2013 NZSEE Conference* (2013).

[13] Mander J B, Panthaki F D, and Kasalanati A, “Low Cycle Fatigue Behavior of Reinforcing Steel”, *Journal of Materials I Civil Engineering, Vol. 6, No.4, Paper No. 6782,* November, 1994.

[14] Koh S.K. and Stephens R.I. 1991. “Mean stress effects on low cycle fatigue for a high strength steel. Fatigue Fracture of Engineering Materials and Structures”, 14(4), 413-428.

[15] “CEB FIP Model Code 90”, *Comite Euro-International Du Beton, Design Code,* 1990.

[16] Roufaiel M.S.L, & Meyer C. (1987a), “Analytical modelling of hysteretic behaviour of R/C frames”, *Journal of Structural Engineering, ASCE*, Vol. 113, No. 3, 429-444.

[17] Wang M.L., & Shah S.P. (1987), Reinforced concrete hysteretic model based on the damage concept, *Earthquake Engineering and Structural Dynamics*, Vol. 15, No. 8, 993-1003

[18] Gosain N.K., Brown R.H. and Jirsa J.O. (1977) Shear requirements for load reversals on RC members, *Journal of Structural Engineering, ASCE*, Vol. 103, No. 7, 1461-1476.

[19] Park Y.J.& Ang A.H-S (1985) Mechanistic seismic damage model for reinforced concrete, *Journal of Structural Engineering, ASCE*, Vol 111, No. ST4, 722-739.

[20] Roufaiel M.S.L, & Meyer C. (1987b), Reliability of concrete frames damaged by earthquakes, *Journal of Structural Engineering, ASCE*, Vol. 113, No. 3, 445-457.

[21] M.J.N. Priestley, G.M. Calvi, M.J. Kowalsky, “Displacement-Based Seismic Design of Structures”, *IUSS Press* 2007

[22] Mander J B, Panthaki F D, and Chaudhary M T, “Evaluation of seismic venerability of highway bridges in the eastern United States.”, (1992), *Lifeline earthquake engineering in the central and eastern U.S., D. B. Ballantyne, ed., ASCE, New York, N.Y.*, Sept., 72-86.

[23] M.S. Williams & R.G. Sexsmith (1995) “Seismic Damage Indices for Concrete Structures: A State-of-the-Art Review”, Earthquake Spectra, Vol. 11, No. 2.